Journal of Medicinal Chemistry

ARTICLE

pubs.acs.org/jmc

Carbonic Anhydrase Activators: Gold Nanoparticles Coated with Derivatized Histamine, Histidine, and Carnosine Show Enhanced Activatory Effects on Several Mammalian Isoforms

Mohamed-Chiheb Saada,[†] Jean-Louis Montero,[†] Daniela Vullo,[‡] Andrea Scozzafava,[‡] Jean-Yves Winum,*[,†] and Claudiu T. Supuran*[,‡]

[†]Institut des Biomolécules Max Mousseron (IBMM), UMR 5247, CNRS-UM1-UM2, Bâtiment de Recherche Max Mousseron, Ecole Nationale Supérieure de Chimie de Montpellier, 8 rue de l'Ecole Normale, 34296 Montpellier Cedex, France

[‡]Università degli Studi di Firenze, Laboratorio di Chimica Bioinorganica, Rm. 188, Via della Lastruccia 3, I-50019 Sesto Fiorentino (Firenze), Italy

ABSTRACT: Lipoic acid moieties were attached to amine or amino acids showing activating properties against the zinc enzyme carbonic anhydrase (CA, EC 4.2.1.1). The obtained lipoic acid conjugates of histamine, L-histidine methyl ester, and L-carnosine methyl ester were attached to gold nanoparticles (NPs) by reaction with Au(III) salts in reducing conditions. The CA activators (CAAs)−coated NPs showed low nanomolar activation (K_As of 1−9 nM) of relevant cytosolic, membrane-bound, mitochondrial, and transmembrane CA isoforms, such as CA I, II, IV, VA, VII, and XIV. These NPs also effectively activated CAs ex vivo, in whole blood experiments, with an increase of 200−280% of the CA activity. This is the first example of enzyme activation with nanoparticles and may lead to biomedical applications for conditions in which the CA activity is diminished, such as aging, Alzheimer's disease, or CA deficiency syndrome.

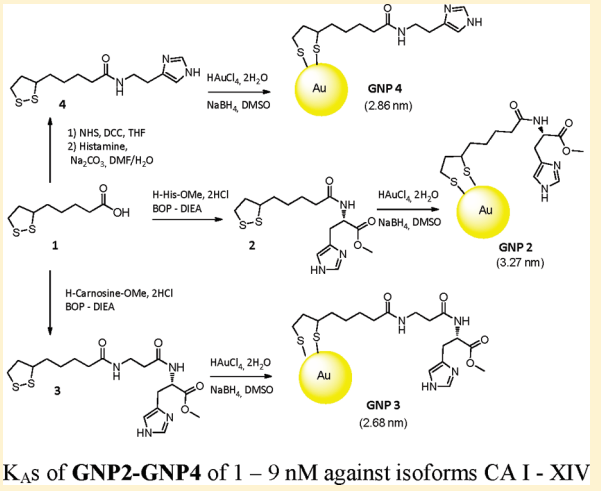

K_As of **GNP2-GNP4** of 1 – 9 nM against isoforms CA I - XIV

INTRODUCTION

In a recent work,[1] we have reported the first nanoparticles (NPs) coated with sulfonamide inhibitors of the metalloenzyme carbonic anhydrase (CA, EC 4.2.1.1). NPs coated with biologically active compounds show interesting biomedical applications both for the site-specific delivery of drugs[2] or for imaging purposes.[2,3] Several recent such examples include HIV inhibition with a CCR5 antagonist attached to multivalent gold nanoparticles, tumor targeting with nanoparticles loaded with hydroxycamptothecin, paclitaxel, or fumagillin, as well as magnetic resonance imaging (MRI) techniques of tumors based on integrins targeting with Fe_3O_4 nanoparticles, computer tomography, or MRI imaging with gadolinium chelate gold nanoparticles, etc.[2] Furthermore, disassembly driven fluorescent nanoprobes for selective protein detection, for various CA isoforms as examples, were recently reported by Hamachi's group.[3] The field of nanoscale enzyme inhibition is also important for better understanding at molecular level drug−protein interactions, as shown for example in a recent work in which fullerene derivatives (the prototypical NP material) were reported to act as efficient CA inhibitors (CAIs)[4] against all physiologically relevant mammalian CA isoforms (16 of which are described so far)[5,6] by means of a novel mechanism of inhibition, i.e., occlusion of the enzyme active site.[4,7]

The CA activators (CAAs), unlike most classes of CAIs, bind at the entrance of the enzyme active site participating in facilitated proton transfer processes between the active site and the reaction medium (the rate determining step of the CA catalytic cycle), as shown by kinetic and X-ray crystallographic work from this and other groups.[8−12] The most extensively investigated CAAs belong to the amine and amino acid class.[8−12] Several high resolution X-ray crystal structures of isoforms CA I and II in adduct with activators such as histamine, L-/D-histidine, L-/D-phenylalanine, D-tryptophan, etc.,[8−12] and synthetic/screening work on various CA isoforms,[13,14] allowed for a rather detailed understanding of the activation mechanism and of the structure−activity relationship governing amine/amino acid type of activators.

The report[15] that some CAAs (such as phenylalanine and imidazole) administered to experimental animals may produce an important pharmacological enhancement of synaptic efficacy,

Received: July 31, 2010
Published: February 03, 2011

Figure 1. Binding of amine and amino acid CAAs to CA II. Superposition of the L-His (gold, PDB 2ABE), D-His (sky blue, PDB 2EZ7), L-Phe (magenta, PDB 2FMG), D-Phe (yellow, PDB 2FMZ), histamine (pink, PDB 1AVN), and D-Trp (gray) adducts. The natural proton shuttle, His64 (in red), the catalytic zinc ion (violet sphere), its three histidine ligands (His94, 96, 119), and the ribbon representation of the protein backbone (green) are also shown.

spatial learning, and memory, proves that this class of relatively unexplored enzyme modulators may have pharmacological applications in conditions in which learning and memory are impaired, such as for example Alzheimer's disease or aging. One must also mention that it was also reported that the levels of CA are significantly diminished in the brain of patients affected by Alzheimer's disease,[16] and these facts strongly support the involvement of different CA isozymes in cognitive functions.[15−17]

Continuing our interest in designing modulators of activity of CAs with compounds/materials possessing a variety of structures, we report here the first nanoscale CAAs, obtained by coating gold nanoparticles (GNPs) with derivatized amine and amino acid activators, and investigate their biological activity against several physiologically relevant CA isoforms.

RESULTS AND DISCUSSION

Chemistry. CAAs bind at the entrance of the enzyme active site cavity,[8] not far away from His64 (Figure 1), the proton shuttle residue of CAs.[9,10] By means of its imidazole moiety and due to its flexibility, this residue shuttles the protons from the zinc bound water molecule to the reaction medium, facilitating thus the formation of the nucleophilic, zinc hydroxide form of the enzyme, which is the catalytically active one.[8,11,12]

As seen from data of Figure 1, CAAs such as histamine,[8a] L- or D-histidine,[12c] and L- or D-phenylalanine[12a] among others, bind at the entrance of the active site cavity, not far away from His64. Their protonatable groups (imidazole, amino, or carboxylate moieties) are able to participate in supplementary proton shuttling processes, leading to an enhanced formation of the nucleophilic species and thus to an activation of the enzyme catalysis. Among the investigated activators, only D-tryptophan binds in a slightly different manner compared to other amines/amino acids,[8b] toward a more external part of the active site, but probably the activation mechanism is the same as for the other compounds mentioned above. The high resolution X-ray crystal structures of hCA II in adduct with all these activators were reported recently.[8,11,12] These and other data[13,14] on compounds synthesized by considering histamine as lead molecule, showed that the histamine/histidine based activators are highly efficient against many CA isoforms with therapeutic applications.[5,6] For example, β-alanyl-L-histidine (L-carnosine) and many of its derivatives were shown earlier to act as effective CAAs.[14a] We considered thus histamine, histidine, and carnosine as lead molecules to design the nanoscale enzyme activators reported in this article.

Similar to the strategy used to prepare NPs coated with sulfonamide CAIs, we employed lipoic acid **1** to derivatize L-His methyl ester, L-carnosine methyl ester, or histamine, obtaining thus the key intermediates **2**−**4** incorporating lipoyl moieties[18] (Scheme 1). The conjugation of **1** with amines/amino acid derivatives occurred by the classical BOP-DIEA chemistry,[18] and the obtained conjugates **2**−**4** were subsequently treated with Au(III) salts in the presence of reducing agents (sodium borohydride) leading to the GNPs of types **GNP2**−**GNP4**, coated with CAAs (L-His methyl ester, **GNP2**, L-carnosine, **GNP3**, and histamine, **GNP4**, respectively) (Scheme 1). The GNPs were characterized extensively (see Experimental Protocols for details) by elemental analysis, EDX analysis, NMR spectroscopy, MS, and TEM analysis. As for the corresponding GNPs coated with sulfonamide CAIs, also **GNP2**−**GNP4** reported here showed diameters in the range of 2.7−3.2 nm (see Experimental Protocols). The ratio between the number of gold atoms and the number of CAA moieties present in the NPs reported here varied between 3:1 and 10.8:1 (see Experimental protocols for details).

As seen from data of Table 1, where the content of gold atoms and activator ligands (L) is presented for three different batches of **GNP2**−**GNP4**, there was a good reproducibility for the preparation of these nano-objects. Indeed, on the basis of the elemental analysis (of gold, nitrogen and sulfur), it was observed that the number of gold atoms varied between 1100 ± 5 for GNP2, between 594 ± 4 for GNP3, and of 722 ± 6 for GNP4. The number of activator molecules present in these nanoparticles (L) were varying in the following way: 366 ± 6 for **GNP2**, 55 ± 2 for **GNP3**, and 178 ± 3 for **GNP4**, respectively. The errors in the concentrations measurements of the stock solution of the activator (of 1 mM) were also estimated by measuring the gold content of an aliquot and are presented in Table 1. These data showed a good reproducibility of the measurements, with errors in the range of 5−10% for the concentration estimation, which are in the same range as those for the stopped flow measurements used to assess the CA activating effects, reported later in this work.

Carbonic Anhydrase Activation. Activation of five physiologically relevant CA isoforms of human (h) origin, i.e., hCA I, II, IV, VA, VII, and XIV, with L-histidine methyl ester, L-carnosine methyl ester, histamine, lipoic acid conjugates **2**−**4**, and nanoparticles **GNP2**−**GNP4**, are shown in Table 2 for the CO_2 hydration reaction catalyzed by these enzymes.[19] Control experiments have also been performed with GNPs containing only the lipoic acid moiety (without amine or amino acid derivatized onto it) of type **GNP5** (prepared in the same conditions as

Table 1. Statistical Analysis of the Gold Nanoparticles GNP2−GNP4 Composition and Concentration Determination, from Three Different Batches Obtained by the Methods Reported in This Paper

	Au[a]		ligand[b]			concentration[c] (mM)	
NP	no. atoms	%	L moieties	% N	% S	calcd	found
GNP2	1100 ± 5	62.31 ± 0.25	366 ± 6	0.050 ± 0.001	0.067 ± 0.001	1.0	1.0 ± 0.04
GNP3	594 ± 4	84.6 ± 0.41	55 ± 2	0.022 ± 0.002	0.025 ± 0.004	1.0	1.0 ± 0.09
GNP4	722 ± 7	72.69 ± 0.32	178 ± 3	0.038 ± 0.002	0.058 ± 0.006	1.0	1.0 ± 0.08

[a] The gold concentration was determined by atomic absorption after dissolution of the nanoparticles in a mixture of concentrated hydrochloric and nitric acid. [b] By combustion. [c] The analytic, calculated concentration was of 1 mM based on the molecular weight of the NPs; the experimental (found) one was assessed based on the gold concentrations, determined as above, for three different batches of each investigated NPs, **GNP2−GNP4**.

Scheme 1. Synthesis of Gold NPs (GNPs) GNP2−GNP4 Incorporating CAAs

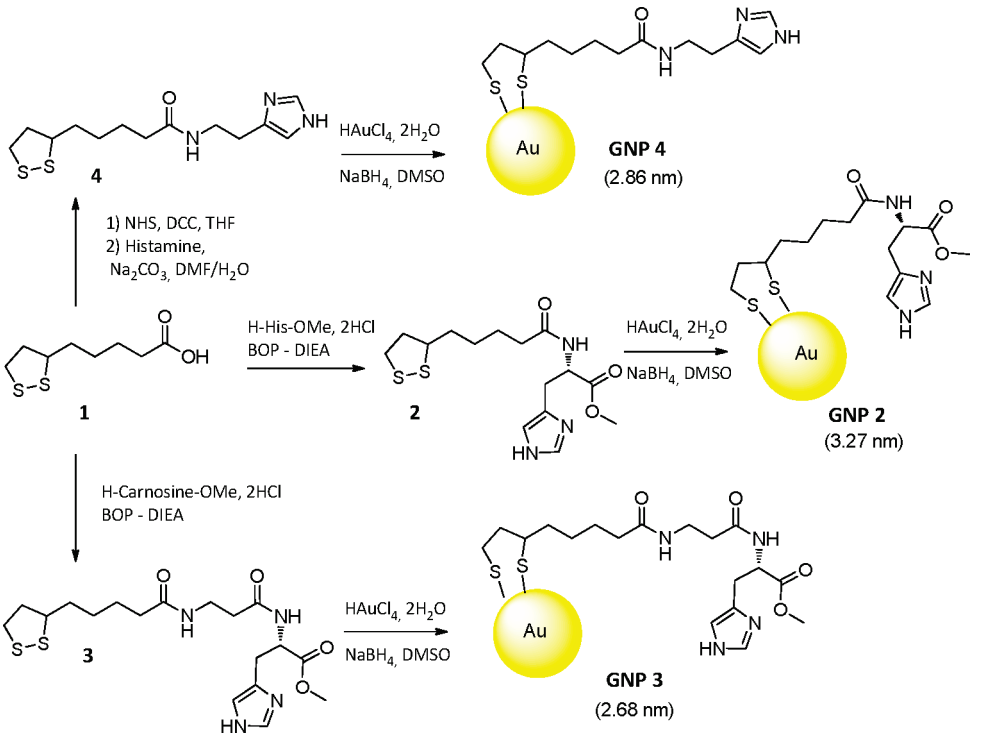

GNP2−GNP4), as well as with a GNP coated with a sulfonamide CAI, reported earlier,[1] **GNP6**.

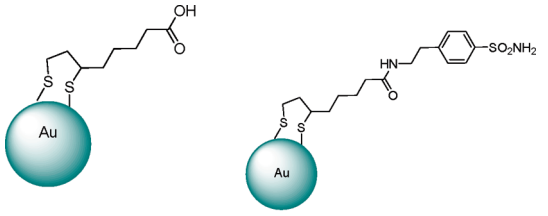

GNP5 **GNP6**

Data of Table 2 show that both L-His and histamine, the two lead compounds used here to design nanoscale enzyme activators, act as CAAs against the six physiologically important isoforms, the cytosolic hCA I, II, and VI, the membrane-associated one hCA IV, the mitochondrial one hCA VA, as well as the transmembrane isoform hCA XIV, all of which are also found in the brain among many other tissues/organs.[20−23] It may be observed that histamine has activation constants in the range of 10 nM to 125 μM against these isoforms,[20] with hCA VA and XIV having the highest affinity and hCA II the lowest affinity for this compound. L-His has an activation profile rather diverse, with K_As in the range of 30 nM to 10.9 μM. The dipeptide L-carnosine has rather similar CA activating properties with L-His, with K_As in the range of 0.64−33.0 μM (Table 2). Derivatization of the last two compounds by esterification of carboxyl moiety with methanol, in the corresponding methyl esters, did not influence significantly the activating properties of the esters compared to the free carboxylic acids from which they were prepared (Table 2). However, the attachment of the lipoyl moiety to these amines/amino acid/dipeptide derivatives lead to compounds **2**−**4** with slightly enhanced CA activating properties compared to the parent compound from which they were prepared. For example, the lipoyl-L-His methyl ester **2** showed K_As in the range of 20 nM to 9.7 μM; the lipoyl L-carnosine methyl ester **3** showed K_As in the range of 0.96−30 μM, whereas lipoyl histamine **4** had these parameters in the range of 13 nM to 116 μM, respectively,

dx.doi.org/10.1021/jm101284a |J. Med. Chem. 2011, 54, 1170–1177

Table 2. Activation of hCA Isozymes I, II, IV, VA, VII, and XIV with L- and D-Histidine, at 25°C, for the CO_2 Hydration Reaction[19]

	K_A[a] (μM)					
isozyme	hCA I[b]	hCA II[b]	hCA IV[c]	hCA VA[d]	hCA VII[b]	hCA XIV[d]
L-His[e]	0.03	10.9	7.3	1.34	0.92	0.90
L-His-OMe	0.02	10.4	6.8	1.86	0.88	0.93
2	0.02	9.7	7.2	1.12	0.78	0.91
GNP2	0.002	0.008	0.001	0.002	0.003	0.001
L-carnosine	1.1	33	19	1.54	0.75	0.64
L-carnosine-OMe	10.9	32	18	1.36	0.84	0.71
3	0.96	30	17	1.25	0.87	0.62
GNP3	0.009	0.007	0.002	0.002	0.001	0.001
histamine[f]	2.1	125	25.3	0.010	37.5	0.010
4	0.77	116	24.1	0.009	35.0	0.013
GNP4	0.005	0.002	0.001	0.001	0.003	0.007
GNP5			inhibition[g]			
GNP6			inhibition[h]			

[a] The activation constant (K_A) for each isozyme was obtained by fitting the observed catalytic enhancements as a function of the activator concentration.[11−14] Mean from at least three determinations by a stopped-flow, CO_2 hydrase method.[19] Standard errors were in the range of 5−10% of the reported values. [b] Human recombinant isozymes. [c] Truncated human recombinant isozyme lacking the first 20 amino acid residues.[26] [d] Full length, human recombinant isoforms.[20−22] [e] From ref 12c. [f] From ref 20. [g] The inhibition constants are in the range of 27−33 μM against the investigated CA isoforms. [h] The inhibition constants are in the range of 2.5−137 nM against the investigated CA isoforms.

against the six investigated CA isoforms (Table 2). The GNPs incorporating either histamine, L-His methyl ester, or L-carnosine methyl ester moieties, **GNP2**−**GNP4**, were on the other hand highly efficient CAAs against all isoforms, with activation constants in the low nanomolar range of 1−9 nM (Table 2). The increase of activating power of the GNPs as compared to the original lead is sometimes dramatic, with factors as high as 62500 for hCA II with **GNP4** and histamine (containing the same CAA moiety), of 12500 for hCA VII (again comparing histamine and the corresponding **GNP4**), etc. This highly increased activating effects observed with the NPs investigated here may be accounted for on the cooperativity effect triggered by the nano-object. Indeed, as there is a rather large number (between 55 and 366) of moieties of the ligand (L) possessing itself activation effects within the reported NP, it is to be expected that these moieties may better act in transferring protons from the enzyme active site to the environment with the assistance of all these multiple proton-shuttling groups present in the nano-object. Furthermore, in the enzyme−activator complex (the case in which the activator is a nanoparticle is discussed here) containing all these multiple proton shuttling moieties, the proton transfer processes become intramolecular,[8] being thus more rapid compared to the intermolecular ones, and this may be an additional effect explaining the high efficiency of these NPs as CAAs.

On the other hand, the GNPs coated only with lipoic acid, **GNP5**, show inhibitory activity against all CA isoforms, similar to the GNPs (Au@) without any derivatization, investigated earlier.[1] Indeed, inhibition constants in the micromolar range have been measured against all isoforms in the presence of **GNP5**. In the case of a GNP derivatized with a sulfonamide CAI, such as **GNP6**, the inhibitory activity is in the nanomolar range against all CA isoforms (Table 2). These data represent a clear proof-of-concept demonstration that it is possible to design not only nanoscale enzyme inhibitors but also nanoscale enzyme activators, a field far less investigated to date. As far as we know, this is the first report in the literature of enzyme activation by NPs.

Table 3. Ex Vivo CA Activation Data after 30 and 60 min of Incubation of Human Erythrocytes with Solutions Containing 0.1−5 μM Activators Investigated Here, Their Lipoic Acid Conjugates and GNPs[a]

	% CA activity[b]	
activator	30 min	60 min
L-His-OMe[c]	137 ± 3	162 ± 9
2[c]	141 ± 8	166 ± 10
GNP2[d]	180 ± 5	245 ± 9
L-carnosine-OMe[c]	131 ± 4	155 ± 8
3[c]	130 ± 6	154 ± 7
GNP3[d]	171 ± 4	263 ± 11
histamine[c]	121 ± 3	130 ± 5
4[c]	125 ± 5	135 ± 7
GNP4[d]	204 ± 12	287 ± 9
GNP5[d]	89 ± 1	87 ± 3
GNP6[d]	11 ± 1	0

[a] Data with **GNP5** and **GNP6** (CAI) are also provided for comparison. [b] Mean ± standard error ($n = 3$); erythrocyte CA activity (hCA I + hCA II) in the absence of activator is taken as 100%. [c] At 5 μM. [d] At 0.1 μM.

Ex Vivo CA Activation. After incubation of normal blood red cells (containing approximately 150 μM of hCA I and 20 μM of hCA II)[24−27] with micromolar concentrations of classical CAAs (histamine, L-carnosine methyl ester, L-histidine methyl ester) or new GNP activators synthesized in the present work (such as **GNP2**, **GNP3**, **GNP4**), the total CA activity in homogenates of treated cells is enhanced as compared to that of cells treated in a blank experiment only with buffer (Table 3). Thus, small molecule CAAs such as L-His-OMe and L-carnosine-OMe produces only a weak-moderate activation of around 120−137% after half an hour incubation and of around 130−162% of the basal CA activity after one hour incubation with red cells. More or less the same effects have been observed with the lipoic acid conjugates of these small molecule CAAs mentioned above, of types **2**−**4**, which produced similar enhancements of the total CA activity after 30 min or 1 h incubation with red blood cells (Table 3). However, some of the new GNPs tested ex vivo (which showed strong in vitro CA activity enhancements, Table 3) of types **GNP2**−**GNP4**, produced much higher activations of 171−204% after half an hour incubation and of 245−287% after one hour incubation (Table 3). As CA is one of the essential buffer systems in biological systems through its production of bicarbonate and protons, a triplicate production of such anions under the effect of an activator as those described here, may be highly relevant. For example, in the CA deficiency syndrome,[25] no CA II is present at all in the body of the affected patients, which has dramatic clinical consequences, such as mental retardation, osteopetrosis, renal calcification, and other life threatening conditions due to the lack of the activity of just one CA isoform. More recently, Birk's and our group[28] reported a single point mutation in the CA XII gene which leads to a protein with 71%

catalytic activity of the wild type one. However, also in this case there were relevant clinical features associated with this genotype, such as hyperchlorohydrosis, mental retardation, delayed development in childhood, etc. Such data show that even a small loss of catalytic activity of one CA isoform may have dramatic clinical consequences. Correction of such a loss with potent activators as those described here may thus have clinical benefit.

As control, we have also performed experiments in which red blood cells have been incubated with the NPs coated only with lipoic acid (**GNP5**) or with a sulfonamide conjugate of lipoic acid (**GNP6**). Data of Table 3 show that **GNP5** produced a weak inhibitory activity on the total blood CA activity (probably due to the gold nanoparticle itself, which is weakly inhibitory against these enzymes).[1] On the other hand, the sulfonamide coated nanoparticles **GNP6** led to a powerful inhibition of the CA activity in red blood cells already after 30 min incubation (an activity of 11% has been measured), whereas a longer incubation, of 1 h, led to the total inhibition of CAs present in red blood cells, as reported earlier for this type of nano-objects.[1] These are clear-cut experiments proving that some of the compounds reported here might act as effective in vivo CA activators and might thus constitute interesting candidates for animal studies regarding their involvement in cognitive processes.

CONCLUSIONS

By attaching lipoic acid moieties to amine or amino acid type CAAs, we prepared lipoic acid conjugates of histamine, L-histidine methyl ester, and L-carnosine methyl ester. Gold nanoparticles were then prepared, coated with these CAAs, which showed low nanomolar activation (K_As of 1−9 nM) of relevant cytosolic, membrane-bound, mitochondrial and transmembrane CA isoforms, such as CA I, II, IV, VA, VII, and XIV. There was a dramatic enhancement of the CA activating properties of the NPs compared to the low molecular activators with comparable structure. The NPs coated with these compounds also effectively activated CA ex vivo, in whole blood experiments, with an increase of 200−280% of the CA activity. This is the first example of enzyme activation with nanoparticles and may lead to biomedical applications.

EXPERIMENTAL PROTOCOLS

General. All reagents and solvents were of commercial quality and used without further purification unless otherwise specified. All reactions were carried out under an inert atmosphere of nitrogen. TLC analyses were performed on silica gel 60 F_{254} plates (Merck Art. 1.05554). Spots were visualized under 254 nm UV illumination or by ninhydrin solution spraying. Melting points were determined o on a Büchi melting point 510 apparatus and are uncorrected. ^{1}H and ^{13}C NMR spectra were recorded on Bruker DRX-400 spectrometer using DMSO-d_6 as solvent and tetramethylsilane as internal standard. For ^{1}H NMR spectra, chemical shifts are expressed in δ (ppm) downfield from tetramethylsilane, and coupling constants (J) are expressed in hertz. Electron Ionization mass spectra were recorded in positive or negative mode on a Water MicroMass ZQ. Transmission electron microscopy (TEM) observations were carried out at 100 kV (JEOL 1200 EXII). Samples for TEM measurements were prepared by dissolving gold NPs suspension in ethanol and placing a drop of the obtained mixture onto a carbon coated copper grip, followed by natural evaporation of the solvent at room temperature. An estimation of the Au/S ratio was performed by using an environmental secondary electron microscope FEI Quanta 200 FEG coupled with an electron dispersive spectroscope Oxford INCA detector. Elemental analysis has been performed by combustion for N and S, and by atomic absorption for Au, after dissolution of the samples in a mixture of fuming hydrochloric and nitric acids (3:1, v/v). Purity of the obtained compounds was assessed by HPLC and elemental analysis (combustion, C, H, N) and was >95% for all of the new derivatives reported here.

Methyl 2-(5-(1,2-Dithiolan-3-yl)pentanamido)-3-(1*H*-imidazol-4-yl)propanoate 2. To a solution of 300 mg of lipoic acid 1 (1.45, 1 equiv) in 5 mL of dimethylacetamide was added 342 mg (1.45 mmol, 1 equiv) of L-histidine methyl ester dihydrochloride, 771 mg (1.74 mmol, 1.2 equiv) of BOP (benzotriazole-1-yl-oxy-tris-(dimethylamino)-phosphonium hexafluorophosphate), and 1 mL (5.81 mmol, 4 equiv) of DIEA. The mixture was stirred overnight at room temperature and then diluted with water and extracted twice by ethyl acetate. The organic layer was dried over anhydrous sodium sulfate and filtered. The filtrate was concentrated under vacuum. The residue was purified on silica gel using a mixture methylene chloride/methanol (90−10, v/v) as eluent; yield 65%; mp 77 °C. R_f = 0.4 (methylene chloride/methanol (90−10, v/v)). ^{1}H NMR (DMSO-d_6, 400 MHz) δ 8.21 (d, 1H, J = 7.6 Hz), 7.71 (s, 1H), 6.86 (s, 1H), 4.48 (td, 1H, J = 8.2 Hz, J = 5.7 Hz), 3.66−3.51 (m, 5H), 3.22−3.13 (m, 1H), 3.13−3.07 (m, 1H), 2.93 (dd, 1H, J = 14.7 Hz, J = 5.5 Hz), 2.84 (dd, 1H, J = 4.7 Hz, J = 8.7 Hz), 2.40 (dq, 1H, J = 12.2 Hz, J = 6.0 Hz), 2.08 (t, 2H, J = 7.2 Hz), 1.92−1.76 (m, 1H), 1.69−1.57 (m, 1H), 1.57−1.38 (m, 3H), 1.34−1.17 (m, 5H). ^{13}C NMR (DMSO-d_6, 101 MHz) δ 172.16, 172.12, 134.77, 132.70, 116.71, 56.12, 56.10, 53.57, 52.13, 51.81, 38.10, 34.80, 34.09, 28.62, 28.12, 28.09, 24.90, 24.89. MS ESI$^+$ m/z 358.20 $[M + H]^+$, 480.18 $[M + Na]^+$. Elemental analysis, found: C, 50.43; H, 6.59; N, 11.60%. $C_{15}H_{23}O_3N_3S_2$ requires: C, 50.20; H, 6.47; N, 11.73%.

*Synthesis of Compound **2** Coated Gold Nanoparticles GNP **2**.* To a solution of 115 mg of $NaBH_4$ and 9 mg of compound **2** in 10 mL of DMSO was added a solution of $HAuCl_4$, $4H_2O$ (80 mg) in 10 mL of DMSO. The reaction mixture turned deep brown immediately. The reaction mixture was stirred at room temperature for 24 h. Then 40 mL of CH_3CN was added to give a black precipitate which was collected by centrifugation, washed two times with 60 mL of acetonitrile and 60 mL of ethanol, and dried under vacuum. EDX and elemental analysis were in agreement with $Au_{1100}(C_{15}H_{23}O_3N_3S_2)_{366}$

TEM Analysis.

Average size of gold nanoparticles **GNP2** = 3.27 nm.

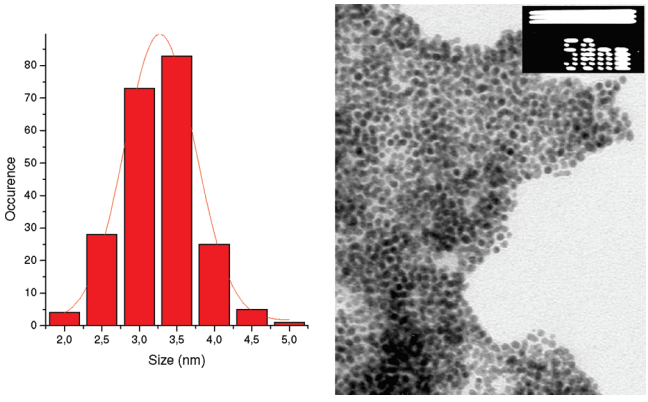

*(2S)-Methyl 2-(3-(5-(1,2-dithiolan-3-yl)pentanamido)propanamido)-3-(4H-imidazol-5-yl)propanoate **3**.* L-Carnosine methyl ester hydrochloride (413 mg, 1.72 mmol, 1.2 equiv) , 771 mg (1.74 mmol, 1.2 equiv) of BOP, and 1 mL (5.81 mmol, 4 equiv) of DIEA were added to a solution of 300 mg of lipoic acid 1 (1.45, 1 equiv) in 5 mL of dimethylacetamide. The mixture was stirred overnight at room temperature and then diluted with water and extracted twice with ethyl acetate. The organic layers were dried over anhydrous sodium sulfate, filtered, and concentrated under vacuum The residue was purified on silica gel using a mixture methylene chloride. methanol (90−10, v/v) as eluent.

Yiel: 75%; mp 56 °C. R_f = 0.29 (methylene chloride/methanol (90−10, v/v)). ^{1}H NMR (DMSO-d_6, 400 MHz) δ 8.31 (d, 1H, J = 7.6 Hz), 7.81(s, 1H), 7.82−7.79 (t, 1H), 4.49 (td, 1H, J = 8.0 Hz, J = 5.8 Hz),

3.65−3.54 (m, 4H), 3.24−3.14 (m, 3H), 3.14−3.08 (m, 1H), 2.96 (dd, 1H, J = 14.7 Hz, J = 5.6 Hz), 2.87 (dd, 1H, J = 14.7 Hz, J = 8.4 Hz), 2.40 (td, 1H, J = 12.6 Hz, J = 6.4 Hz), 2.25 (t, 2H, J = 7.3 Hz), 2.03 (t, 2H, J = 7.4 Hz), 1.85 (m, 1H), 1.71−1.59 (m, 1H), 1.59−1.40 (m, 3H), 1.38−1.28 (m, 2H), 1.28−1.21 (m, 2H). ^{13}C NMR (DMSO-d_6, 101 MHz) δ 171.98, 171.89, 170.49, 134.68, 132.35, 116.59, 56.07, 54.86, 52.08, 51.84, 39.87, 38.04, 35.09, 35.04, 34.07, 28.34, 28.27, 24.95. MS ESI$^+$ m/z 429.20 $[M + H]^+$, 451.19 $[M + Na]^+$, ESI$^-$ m/z 387.18 $[M - H]^-$. Elemental analysis, found: C, 55.62; H, 7.12; N, 14.31%. $C_{18}H_{28}O_4N_4S_2$ requires: C, 55.83; H, 7.28; N, 14.47%.

*Synthesis of CAA-Carnosine Coated Gold Nanoparticles GNP **3**.* To a solution of 115 mg of $NaBH_4$ and 14 mg of compound **3** in 10 mL of DMSO was added a solution of $HAuCl_4$,$4H_2O$ (80 mg) in 10 mL of DMSO. The reaction mixture turned deep brown immediately. The reaction mixture was stirred at room temperature for 24 h. Then 40 mL of CH_3CN was added to give a black precipitate which was collected by centrifugation, washed two times with 60 mL of acetonitrile and 60 mL of ethanol, and dried under vacuum. EDX and Elemental analysis were in agreement with $[Au_{594}(C_{18}H_{28}O_4N_4S_2)_{55}]$

TEM Analysis.

Average size of gold nanoparticles **GNP3** = 2.68 nm.

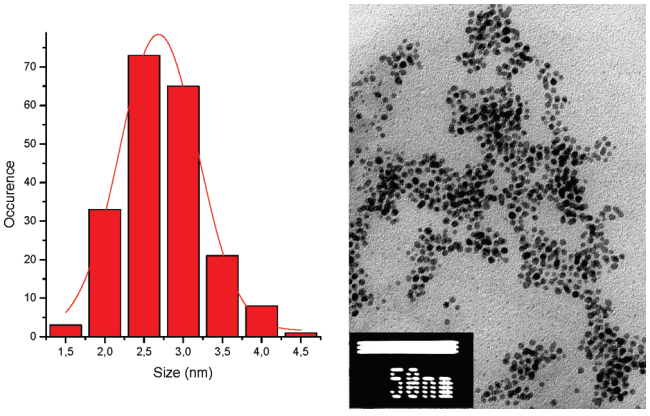

*N-(2-(1H-Imidazol-4-yl)ethyl)-5-(1,2-dithiolan-3-yl)pentanamide **4**.* A solution of 250 mg of lipoate−NHS ester (0.82 mmol, 1.1 equiv) (prepared as described by Liu et al.[26]) in 4 mL of DMF was added dropwise over 10 min to a solution of 83 mg of histamine (0.75 mmol, 1equiv) and 63 mg of sodium bicarbonate (0.75 mmol, 1 equiv) in DMF/water (6 mL, 1:1 v/v) at 0 °C. The solution was stirred under reflux overnight. The mixture was then extracted with chloroform (3 × 10 mL). The combined organic extracts were washed with water (3 × 10 mL), dried over anhydrous Na_2SO_4, filtered, and concentrated under vacuum. The crude product was purified on silica gel using a mixture methylene chloride. methanol (90−10, v/v) as eluent to give the final product as a yellow solid; yield 60%; mp 98 °C; R_f = 0.32 (methylene chloride/methanol (90−10, v/v)). ^{1}H NMR (DMSO-d_6, 400 MHz) δ 7.86 (t, 1H, J = 5.4 Hz), 7.52 (s, 1H), 6.77 (s, 1H), 3.60 (dt, 2H, J = 14.8 Hz, J = 6.2 Hz), 3.24 (dd, 3H, J = 13.3 Hz, J = 7.3 Hz), 3.21 − 3.06 (m, 3H), 2.60 (t, 2H, J = 5.9 Hz), 2.40 (td, 1H, J = 12.4 Hz, J = 6.2 Hz), 2.04 (t, 2H, J = 7.3 Hz), 1.85 (dq, 1H, J = 13.5 Hz, J = 6.8 Hz), 1.65 (m, 1H), 1.59−1.42 (m, 3H), 1.38−1.26 (m, 2H). ^{13}C NMR (DMSO-d_6, 101 MHz) δ 171.81, 134.55, 56.09, 38.58, 38.06, 35.18, 34.08, 28.26, 26.96, 25.01. MS ESI$^+$ m/z 300.20 $[M + H]^+$, 322.30 $[M + Na]^+$. Elemental analysis, found: C, 52.13; H, 6.79; N, 13.67%. $C_{13}H_{21}ON_3S_2$ requires: C, 52.00; H, 7.05; N, 14.00%.

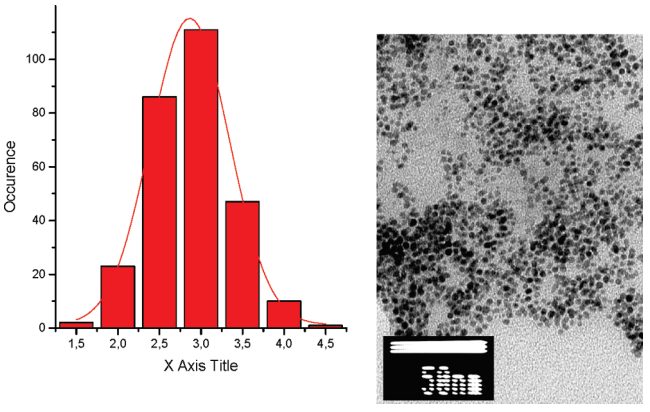

*Synthesis of Histamine Coated Gold Nanoparticles GNP**4**.* To a solution of 115 mg of $NaBH_4$ and 9 mg of compound **4** in 10 mL of DMSO was added a solution of $HAuCl_4$ and $4H_2O$ (80 mg) in 10 mL of DMSO. The reaction mixture turned deep brown immediately. The reaction mixture was stirred at room temperature for 24 h. Then 40 mL of CH_3CN was added to give a black precipitate which was collected by centrifugation, washed two times with 60 mL of acetonitrile and 60 mL of ethanol, and dried under vacuum. EDX and elemental analysis were in agreement with $[Au_{722}(C_{13}H_{21}ON_3S_2)_{178}]$.

TEM Analysis.

Average size of gold nanoparticles **GNP4** = 2.86 nm.

CA Assay. A stopped-flow method[19] has been used for assaying the CA catalyzed CO_2 hydration activity with Phenol Red as indicator, working at the absorbance maximum of 557 nm, following the initial rates of the CA-catalyzed CO_2 hydration reaction for 10−100 s. For each activator at least six traces of the initial 5−10% of the reaction have been used for determining the initial velocity. The uncatalyzed rates were determined in the same manner and subtracted from the total observed rates. Stock solutions of activator (0.01 mM) were prepared in distilled−deionized water with 5% DMSO, and dilutions up to 0.01 nM were done thereafter with distilled−deionized water. The nanoparticles were totally soluble in this solvent mixture. Activator (concentration range 0.01 μM to 0.01 nM) and enzyme solutions ([E] = 10 nM) were preincubated together for 15 min to 2 h at room temperature prior to assay in order to allow for the formation of the E−A complex. The activation constant (K_A), defined similarly with the inhibition constant K_I,[8,11−14] can be obtained by considering the classical Michaelis−Menten equation (eq 1), which has been fitted by nonlinear least-squares by using PRISM 3:

$$v = v_{max}/\{1+K_M/[S](1+[A]_f/K_A)\} \quad (1)$$

where $[A]_f$ is the free concentration of activator.

Working at substrate concentrations considerably lower than K_M ($[S] \ll K_M$), and considering that $[A]_f$ can be represented in the form of the total concentration of the enzyme ($[E]_t$) and activator ($[A]_t$), the obtained competitive steady-state equation for determining the activation constant is given by eq 2:[11−14]

$$v = v_0 \cdot K_A/\{K_A+([A]_t-0.5\{([A]_t+[E]_t+K_A)-([A]_t+[E]_t+K_A)^2 -4[A]_t\cdot[E]_t)^{1/2}\}\} \quad (2)$$

where v_0 represents the initial velocity of the enzyme-catalyzed reaction in the absence of activator.[11−14] All CA isozymes used in the experiments were purified recombinant proteins obtained as reported by our group.[1,12,14]

Ex Vivo CA Activation. An amount of 2 mL of freshly isolated human blood was thoroughly washed several times with 5 mL of Tris buffer (pH 7.40, 5 mM) and centrifuged for 10 min. The obtained erythrocytes were then treated with 2 mL of a 0.1−5 μM solution of CA activator. Incubation has been done at 37 °C with gentle stirring for periods of 30−60 min. After that time, the red cells were centrifuged again for 10 min, the supernatant discarded, and the cells washed three times with 5 mL of the above-mentioned buffer in order to eliminate all unbound activator. The cells were then lysed in 5 mL of distilled water, centrifuged for eliminating membranes and other insoluble materials, and CA activity was assayed as

described above.[19] Blank experiments were done in which no activator has been added to the blood red cells treated as described above, and CA activity determined in such conditions has been taken as 100%.[27]

AUTHOR INFORMATION

Corresponding Author

*For J.-Y.W.: E-mail, jean-yves.winum@univ-montp2.fr. For C.T.S.: phone, 39-055-4573005; fax, 39-055-4573385; E-mail, claudiu.supuran@unifi.it.

ACKNOWLEDGMENT

This research was financed in part by a grant of the 7th Framework Programme of the European Union (Metoxia project, to C.T.S. and A.S.) and by the grant CNRS MIE-2007 (Programme "Maladies Infectieuses Emergentes" Centre National de la Recherche Scientifique, France, to J.-Y.W).

ABBREVIATIONS USED

BOP, benzotriazole-1-yl-oxy-tris-(dimethylamino)-phosphonium hexa-fluorophosphate; CA, carbonic anhydrase; CAA, CA activator; CAI, CA inhibitor; DIEA, diisopropylethylamine; EDX, energy dispersive X-ray analysis; GNP, gold nanoparticle; MRI, magnetic resonance imaging; NP, nanoparticle; TEM, transmission electron microscopy

REFERENCES

(1) Stiti, M.; Cecchi, A.; Rami, M.; Abdaoui, M.; Barragan-Montero, V.; Scozzafava, A.; Guari, Y.; Winum, J. Y.; Supuran, C. T. Carbonic anhydrase inhibitor coated gold nanoparticles selectively inhibit the tumor-associated isoform IX over the cytosolic ubiquitous isozymes I and II. *J. Am. Chem. Soc.* **2008**, *130*, 16130–16131.

(2) (a) Bowman, M. C.; Ballard, T. E.; Ackerson, C. J.; Feldheim, D. L.; Margolis, D. M.; Melander, C. Inhibition of HIV fusion with multivalent gold nanoparticles. *J. Am. Chem. Soc.* **2008**, *130*, 6896–6897. (b) Xie, J.; Chen, K.; Lee, H. Y.; Xu, C.; Hsu, A. R.; Peng, S.; Chen, X.; Sun, S. Ultrasmall c(RGDyK)-coated Fe_3O_4 nanoparticles and their specific targeting to integrin alpha(v)beta3-rich tumor cells. *J. Am. Chem. Soc.* **2008**, *130*, 7542–7543. (c) Ansell, S. M.; Johnstone, S. A.; Tardi, P. G.; Lo, L.; Xie, S.; Shu, Y.; Harasym, T. O.; Harasym, N. L.; Williams, L.; Bermudes, D.; Liboiron, B. D.; Saad, W.; Prud'homme, R. K.; Mayer, L. D. Modulating the therapeutic activity of nanoparticle delivered paclitaxel by manipulating the hydrophobicity of prodrug conjugates. *J. Med. Chem.* **2008**, *51*, 3288–3296.

(3) Mizusawa, K.; Ishida, Y.; Takaoka, Y.; Miyagawa, M.; Tsukiji, S.; Hamachi, I. Disassembly-driven turn-on fluorescent nanoprobes for selective protein detection. *J. Am. Chem. Soc.* **2010**, *132*, 7291–7293.

(4) Innocenti, A.; Durdagi, S.; Doostdar, N.; Strom, T. A.; Barron, A. R.; Supuran, C. T. Nanoscale enzyme inhibitors: fullerenes inhibit carbonic anhydrase by occluding the active site entrance. *Bioorg. Med. Chem.* **2010**, *28*, 2822–2828.

(5) (a) Supuran, C. T. Carbonic anhydrases: novel therapeutic applications for inhibitors and activators. *Nature Rev. Drug Discovery* **2008**, *7*, 168–181. (b) Supuran, C. T. Carbonic anhydrase inhibitors. *Bioorg. Med. Chem. Lett.* **2010**, *20*, 3467–3474. (c) Supuran, C. T. Carbonic anhydrases as drug targets—general presentation. In *Drug Design of Zinc−Enzyme Inhibitors: Functional, Structural, and Disease Applications*; Supuran, C. T., Winum, J. Y., Eds.; Wiley: Hoboken, NJ, 2009; pp 15−38. (d) Barrese, A. A., III; Genis, C.; Fisher, S. Z.; Orwenyo, J. N.; Kumara, M. T.; Dutta, S. K.; Phillips, E.; Kiddle, J. J.; Tu, C.; Silverman, D. N.; Govindasamy, L.; Agbandje-McKenna, M.; McKenna, R.; Tripp, B. C. Inhibition of carbonic anhydrase II by thioxolone: a mechanistic and structural study. *Biochemistry* **2008**, *47*, 3174–3179.

(6) (a) Domsic, J. F.; Avvaru, B. S.; Kim, C. U.; Gruner, S. M.; Agbandje-McKenna, M.; Silverman, D. N.; McKenna, R. Entrapment of carbon dioxide in the active site of carbonic anhydrase II. *J. Biol. Chem.* **2008**, *283*, 30766–307681. (b) Fisher, S. Z.; Maupin, C. M.; Budayova-Spano, M.; Govindasamy, L.; Tu, C. K.; Agbandje-McKenna, M.; Silverman, D. N.; Voth, G. A.; McKenna, R. Atomic crystal and molecular dynamics simulation structures of human carbonic anhydrase II: insights into the proton transfer mechanism. *Biochemistry* **2007**, *42*, 2930–2937. (c) Winum, J. Y.; Rami, M.; Scozzafava, A.; Montero, J. L.; Supuran, C. Carbonic Anhydrase IX: a new druggable target for the design of antitumor agents. *Med. Res. Rev.* **2008**, *28*, 445–463. (d) Supuran, C. T.; Scozzafava, A.; Casini, A. Carbonic Anhydrase Inhibitors. *Med. Res. Rev.* **2003**, *23*, 146–189.

(7) Maresca, A.; Temperini, C.; Vu, H.; Pham, N. B.; Poulsen, S. A.; Scozzafava, A.; Quinn, R. J.; Supuran, C. T. Non-zinc mediated inhibition of carbonic anhydrases: coumarins are a new class of suicide inhibitors. *J. Am. Chem. Soc.* **2009**, *131*, 3057–3062.

(8) (a) Briganti, F.; Mangani, S.; Orioli, P.; Scozzafava, A.; Vernaglione, G.; Supuran, C. T. Carbonic anhydrase activators: X-ray crystallographic and spectroscopic investigations for the interaction of isozymes I and II with histamine. *Biochemistry* **1997**, *36*, 10384–10392. (b) Temperini, C.; Innocenti, A.; Scozzafava, A.; Supuran, C. T. Carbonic anhydrase activators. Kinetic and X-ray crystallographic study for the interaction of D- and L-tryptophan with the mammalian isoforms I−XIV. *Bioorg. Med. Chem.* **2008**, *16*, 8373–8378. (b) Temperini, C.; Scozzafava, A.; Puccetti, L.; Supuran, C. T. Carbonic anhydrase activators: X-ray crystal structure of the adduct of human isozyme II with L-histidine as a platform for the design of stronger activators. *Biorg. Med. Chem. Lett.* **2005**, *15*, 5136–5141.

(9) (a) Tu, C. K.; Silverman, D. N.; Forsman, C.; Jonsson, B. H.; Lindskog, S. Role of histidine 64 in the catalytic mechanism of human carbonic anhydrase II studied with a site-specific mutant. *Biochemistry* **1989**, *28*, 7913–7918. (b) Behravan, G.; Jonasson, P.; Jonsson, B. H.; Lindskog, S. Structural and functional differences between carbonic anhydrase isoenzymes I and II as studied by site-directed mutagenesis. *Eur. J. Biochem.* **1991**, *198*, 589–592. (c) Engstrand, C.; Jonsson, B. H.; Lindskog, S. *Eur. J. Biochem.* **1995**, *229*, 696–702. (d) Almstedt, K.; Rafstedt, T.; Supuran, C. T.; Carlsson, U.; Hammarström, P. Small-molecule suppression of misfolding of mutated human carbonic anhydrase II linked to marble brain disease. *Biochemistry* **2009**, *48*, 5358–5364.

(10) (a) Elder, I.; Han, S.; Tu, C.; Steele, H.; Laipis, P. J.; Viola, R. E.; Silverman, D. N. Activation of carbonic anhydrase II by active-site incorporation of histidine analogs. *Arch. Biochem. Biophys.* **2004**, *421*, 283–289. (b) Liang, Z.; Xue, Y.; Behravan, G.; Jonsson, B. H.; Lindskog, S. Importance of the conserved active-site residues Tyr7, Glu106, and Thr199 for the catalytic function of human carbonic anhydrase II. *Eur. J. Biochem.* **1993**, *211*, 821–827.

(11) (a) Temperini, C.; Scozzafava, A.; Supuran, C. T. Carbonic anhydrase activation and the drug design. *Curr. Pharm. Des.* **2008**, *14*, 708–715. (b) Ilies, M.; Scozzafava, A.; Supuran, C. T. Carbonic anhydrase activators. In *Carbonic Anhydrase—Its Inhibitors and Activators*, Supuran, C. T.; Scozzafava, A.; Conway, J., Eds., CRC Press: Boca Raton FL, 2004; pp 317−352; (c) Supuran, C. T.; Scozzafava, A. Activation of carbonic anhydrase isozymes. In *The Carbonic Anhydrases—New Horizons*; Chegwidden, W. R., Carter, N., Edwards, Y., Eds.; Birkhauser Verlag: Basel, Switzerland, 2000; pp 197−219 ;(d) Temperini, C.; Innocenti, A.; Scozzafava, A.; Mastrolorenzo, A.; Supuran, C. T. Carbonic anhydrase activators: L-adrenaline plugs the active site entrance of isozyme II, activating better isoforms I, IV, VA, VII, and XIV. *Bioorg. Med. Chem. Lett.* **2007**, *17*, 628–635.

(12) (a) Temperini, C.; Vullo, D.; Scozzafava, A.; Supuran, C. T. Carbonic anhydrase activators. Activation of isoforms I, II, IV, VA, VII, and XIV with L- and D-phenylalanine and crystallographic analysis of their adducts with isozyme II: sterospecific recognition within the active site of an enzyme and its consequences for the drug design. *J. Med. Chem.* **2006**, *49*, 3019–3027. (b) Nishimori, I.; Onishi, S.; Vullo, D.; Innocenti, A.; Scozzafava, A.; Supuran, C. T. Carbonic anhydrase activators. The first activation study of the human secretory isoform VI. *Bioorg. Med.*

Chem. **2007**, *15*, 5351–5357. (c) Temperini, C.; Scozzafava, A.; Vullo, D.; Supuran, C. T. Carbonic anhydrase activators. Activation of isozymes I, II, IV, VA, VII, and XIV with L- and D-histidine and crystallographic analysis of their adducts with isoform II: engineering proton transfer processes within the active site of an enzyme. *Chemistry* **2006**, *12*, 7057–7066. (d) Pastorekova, S.; Vullo, D.; Nishimori, I.; Scozzafava, A.; Pastorek, J.; Supuran, C. T. Carbonic anhydrase activators. Activation of the human tumor-associated isozymes IX and XII with amino acids and amines. *Bioorg. Med. Chem.* **2008**, *16*, 3530–3536. (e) Abdo, M.-R.; Vullo, D.; Saada, M.-C.; Montero, J.-L.; Scozzafava, A.; Winum, J.-Y.; Supuran, C. T. Carbonic anhydrase activators: activation of human isozymes I, II, and IX with phenylsulfonylhydrazido L-histidine derivatives. *Bioorg. Med. Chem. Lett.* **2009**, *19*, 2440–2443.

(13) (a) Briganti, F.; Scozzafava, A.; Supuran, C. T. Novel carbonic anhydrase isozymes I, II, and IV activators incorporating sulfonylhistamino moieties. *Bioorg. Med. Chem. Lett.* **1999**, *9*, 2043–2048. (b) Supuran, C. T.; Scozzafava, A. Carbonic anhydrase activators. Amino acyl/dipeptidyl histamine derivatives bind with high affinity to isozymes I, II, and IV and act as efficient activators. *Bioorg. Med. Chem.* **1999**, *7*, 2915–2924. (c) Scozzafava, A.; Supuran, C. T. Carbonic anhydrase activators. Part 24. High affinity isozymes I, II and IV activators, derivatives of 4-(4-chlorophenylsulfonylureido-amino acyl)ethyl-1*H*-imidazole. *Eur. J. Pharm. Sci.* **2000**, *10*, 29–41. (d) Scozzafava, A.; Iorga, B.; Supuran, C. T. Carbonic anhydrase activators. (Part 22) Synthesis of high affinity isozymes I, II and IV activators, derivatives of 4-(4-tosylureido-amino acyl)ethyl-1*H*-imidazole (histamine derivatives). *J. Enzyme Inhib.* **2000**, *15*, 139–161.

(14) (a) Scozzafava, A.; Supuran, C. T. Carbonic anhydrase activators: high affinity isozymes I, II and IV activators, incorporating a β-alanyl-histidine scaffold. *J. Med. Chem.* **2002**, *45*, 284–291. (b) Scozzafava, A.; Supuran, C. T. Carbonic anhydrase activators: human isozyme II is strongly activated by oligopeptides incorporating the carboxyterminal sequence of the bicarbonate anion exchanger AE1. *Bioorg. Med. Chem. Lett.* **2002**, *12*, 1177–1180. (c) Ilies, M.; Banciu, M. D.; Ilies, M. A.; Scozzafava, A.; Caproiu, M. T.; Supuran, C. T. Carbonic anhydrase activators: design of high affinity isozymes I, II, and IV activators, incorporating tri-/tetrasubstituted-pyridinium-azole moieties. *J. Med. Chem.* **2002**, *45*, 504–510.

(15) (a) Sun, M. K.; Alkon, D. L. Pharmacological enhancement of synaptic efficacy, spatial learning and memory through carbonic anhydrase activation in rats. *J. Pharmacol. Exp. Ther.* **2001**, *297*, 961–967. (b) Sun, M.-K.; Alkon, D. L. Carbonic anhydrase gating of attention: memory therapy and enhancement. *Trends Pharmacol. Sci.* **2002**, *23*, 83–92.

(16) (a) Meier-Ruge, W.; Iwangoff, P.; Reichlmeier, K. Neurochemical enzyme changes in Alzheimer's and Pick's disease. *Arch. Gerontol. Geriatr.* **1984**, *3*, 161–165. (b) Lakkis, M. M.; O'Shea, K. S.; Tashian, R. E. Differential expression of the carbonic anhydrase genes for CA VII (Car7) and CA-RP VIII (Car8) in mouse brain. *J. Histochem. Cytochem.* **1997**, *45*, 657–662.

(17) (a) Sultana, R.; Boyd-Kimball, D.; Poon, H. F.; Cai, J.; Pierce, W. M.; Klein, J. B.; Merchant, M.; Markesbery, W. R.; Butterfield, D. A. Redox proteomics identification of oxidized proteins in Alzheimer's disease hippocampus and cerebellum: an approach to understand pathological and biochemical alterations in AD. *Neurobiol. Aging* **2006**, *22*, 76–87. (b) Korolainen, M. A.; Goldsteins, G.; Nyman, T. A.; Alafuzoff, I.; Koistinaho, J.; Pirttila, T. Oxidative modification of proteins in the frontal cortex of Alzheimer's disease brain. *Neurobiol. Aging* **2006**, *27*, 42–53. (c) Poon, H. F.; Frasier, M.; Shreve, N.; Calabrese, V.; Wolozin, B.; Butterfield, D. A. Mitochondrial associated metabolic proteins are selectively oxidized in A30P α-synuclein transgenic mice—a model of familial Parkinson's disease. *Neurobiol. Dis.* **2005**, *18*, 492–498.

(18) Daniel, M. C.; Astruc, D. Gold nanoparticles: assembly, supramolecular chemistry, quantum-size-related properties, and applications toward biology, catalysis, and nanotechnology. *Chem. Rev.* **2004**, *104*, 293–346.

(19) Khalifah, R. G. The carbon dioxide hydration activity of carbonic anhydrase. I. Stop-flow kinetic studies on the native human isoenzymes B and C. *J. Biol. Chem.* **1971**, *246*, 2561–73.

(20) (a) Vullo, D.; Innocenti, A.; Nishimori, I.; Scozzafava, A.; Kaila, K.; Supuran, C. T. Carbonic anhydrase activators. Activation of the human isoforms VII (cytosolic) and XIV (transmembrane) with amino acids and amines. *Bioorg. Med. Chem. Lett.* **2007**, *17*, 4107–4112. (b) Vullo, D.; Nishimori, I.; Innocenti, A.; Scozzafava, A.; Supuran, C. T. Carbonic anhydrase activators. An activation study of the human mitochondrial isoforms VA and VB with amino acids and amines. *Bioorg. Med. Chem. Lett.* **2007**, *17*, 1336–1340. (c) Vullo, D.; Nishimori, I.; Scozzafava, A.; Supuran, C. T. Carbonic anhydrase activators. Activation of the human cytosolic isozyme III and membrane-associated one IV with amino acids and amines. *Bioorg. Med. Chem. Lett.* **2008**, *18*, 4303–4307.

(21) Pastorekova, S.; Parkkila, S.; Pastorek, J.; Supuran, C. T. Carbonic anhydrases: current state of the art, therapeutic applications and future prospects. *J. Enzyme Inhib. Med. Chem.* **2004**, *19*, 199–229.

(22) Supuran, C. T.; Scozzafava, A. Carbonic anhydrase activators as potential anti-Alzheimer's disease agents. In *Protein Misfolding in Neurodegenerative Diseases: Mechanisms and Therapeutic Strategies*; Smith, H. J., Simons, C., Sewell, R. D. E., Eds., CRC Press: Boca Raton, FL, 2007; pp 265−288.

(23) Masseguin, C.; LePanse, S.; Corman, B.; Verbavatz, J. M.; Gabrion, J. Aging affects choroidal proteins involved in CSF production in Sprague−Dawley rats. *Neurobiol. Aging* **2005**, *26*, 917–927.

(24) Wistrand, P. J., Lindqvist, A. Design of carbonic anhydrase inhibitors and the relationship between the pharmacodynamics and pharmacokinetics of acetazolamide. In *Carbonic Anhydrase—From Biochemistry and Genetics to Physiology and Clinical Medicine*.; Botrè, F., Gros, G., Storey, B. T., Eds.; VCH: New York—Weinheim, 1991; pp 352−378.

(25) Sly, W. S. Carbonic anhydrase II deficiency syndrome: clinical delineation, interpretation and implications. In *The Carbonic Anhydrases*; Dodgson, S. J., Tashian, R. E., Gros, G., Carter, N. D., Eds.; Plenum Press: New York, London, 1991; pp 183−196.

(26) Liu, W.; Howarth, M.; Greytak, A. B.; Zheng, Y.; Nocera, D. G.; Ting, A. Y.; Bawendi, M. G. Compact biocompatible quantum dots functionalized for cellular imaging. *J. Am. Chem. Soc.* **2008**, *130*, 1274–1284.

(27) Scozzafava, A.; Briganti, F.; Ilies, M. A.; Supuran, C. T. Carbonic anhydrase inhibitors. Synthesis of membrane-impermeant low molecular weight sulfonamides possessing in vivo selectivity for the membrane-bound versus the cytosolic isozymes. *J. Med. Chem.* **2000**, *43*, 292–300.

(28) Feldshtein, M.; Elkrinawi, S.; Yerushalmi, B.; Marcus, B.; Vullo, D.; Romi, H.; Ofir, R.; Landau, D.; Sivan, S.; Supuran, C. T.; Birk, O. S. Hyperchlorhidrosis caused by homozygous mutation in CA12, encoding carbonic anhydrase XII. *Am. J. Hum. Genet.* **2010**, *87*, 713–720.